Thin Solid Films 519 (2011) 7444–7448

Contents lists available at ScienceDirect

Thin Solid Films

journal homepage: www.elsevier.com/locate/tsf

The use of aluminium doped ZnO as transparent conductive oxide for CdS/CdTe solar cells

J. Perrenoud *, L. Kranz, S. Buecheler, F. Pianezzi, A.N. Tiwari

Empa, Swiss Federal Laboratories for Materials Science and Technology, Laboratory for Thin Films and Photovoltaics, Überlandstrasse 129, 8600 Dübendorf, Switzerland

ARTICLE INFO

Available online 15 January 2011

Keywords:
CdTe
ZnO
TCO
Intrinsic ZnO

ABSTRACT

CdTe/CdS and CdTe/ZnO thin film solar cells were grown with a high vacuum evaporation based low temperature process (≤420 °C). Aluminium doped zinc oxide (AZO) was used as transparent conducting oxide (TCO) material. AZO exhibited excellent stability during the solar cell processing, and no significant change in electrical conductivity or transparency was observed. The current density loss due to absorption in the 1 μm thick AZO layer with 5 Ω per square sheet resistance was found to be 1.2 mA/cm^2. We investigated the influence of an intrinsic ZnO layer (i:ZnO) in combination with various CdS thicknesses. The i:ZnO layer was found to significantly increase the open circuit voltage of the solar cells with very thin CdS layer. Increasing thickness of the i:ZnO layer leads to UV absorption losses, narrowing of the depletion layer width and hence reduced collection efficiency in the long wavelength (685–830 nm) part. With AZO/i:ZnO bi-layer TCO we could achieve cell efficiencies of 15.6% on glass and 12.4% on the flexible polyimide film.

1. Introduction

Important requirements for the transparent conductive oxide (TCO) as an electrical front contact in highly efficient solar cells are high energy band gap (E_g^{TCO}), low absorption for photon energy below E_g^{TCO}, low free carrier absorption, high in-plane conductivity and sufficient stability under the conditions for subsequent deposition processes and total lifetime of the device. When CdS layer thickness is reduced for absorption loss minimisation direct contact between CdTe and the TCO can happen because of non-conformal coverage; hence electronic features like conduction band offset between the window layer and the CdTe can be important.

Commonly used materials for transparent electrodes are SnO_x doped with fluorine (FTO), In_2O_3 doped with tin (ITO), cadmium stannate (CTO) and ZnO doped with aluminium (AZO). FTO is commonly used in CdS/CdTe thin film solar cells. The application of AZO as TCO in CdS/CdTe solar cells was reported by Gupta and Compaan in all-sputtered devices with 14.0% efficiency [1]. We present here the utilization of AZO in high vacuum evaporated CdS/CdTe thin films on various substrates. Results of the detailed investigation on the influence of an intermediate intrinsic ZnO (i:ZnO) layer is also presented in this paper.

2. Experimental details

The solar cells were grown on borosilicate glass (BSG), aluminosilicate glass (ASG), soda lime glass (SLG) or flexible polyimide (PI) film substrates. The TCO used was AZO followed by an i:ZnO layer in some cases. Both layers were deposited at a substrate temperature of 300 °C by RF magnetron sputtering. The sputtering system used for both, the AZO and the i:ZnO layer, was a vacuum chamber made by AJA international, Inc., with A360 magnetrons with 4 inch ceramic targets. The CdS and CdTe layers were deposited in a high vacuum evaporation system. The substrate temperature was 165 °C and 350 °C respectively during the layer depositions. Before CdTe deposition the CdS is annealed at about 450°C in order to enhance crystallisation of the CdS layer. The activation treatment was performed by depositing 400 nm $CdCl_2$ and subsequent annealing in air at 420 °C. The back contact was formed by etching the surface in a dilute (0.1%) bromine methanol solution before the deposition of Cu (about 2.5 nm) and Au (about 40 nm) layers. In order to enhance the Cu_xTe formation the finished device is annealed at 200 °C. The conductivity of the TCO layer was measured via silver line contacts which were deposited between the substrate and the TCO at two opposite borders. This allowed measuring the resistivity after every processing step and also in the final device via a two point probe (the contribution of the other layers can be neglected due to high in-plane resistivity). The solar cells were characterized by current–voltage (J–V) and spectral response (SR) measurements according to the international standards IEC 60904-1 Ed. 2 and IEC 60904-8 Ed. 2. From SR measurements the external quantum efficiency (EQE) and the short circuit current density under AM1.5 (J_{SC} [AM1.5]) were calculated with the reference

* Corresponding author. Tel.: +41 44 823 61 06.
E-mail address: julian.perrenoud@empa.ch (J. Perrenoud).

0040-6090/$ – see front matter © 2011 Elsevier B.V. All rights reserved.
doi:10.1016/j.tsf.2010.12.234

spectrum from IEC 60904-4 Ed.2. Transmission and reflection measurements were performed with a Shimadzu UV 3600 spectrometer. Capacitance–voltage (C–V) and capacitance–frequency (C–f) measurements were done with an E4980A Precision LCR Meter from Agilent while controlling the cell temperature in a home made cryostat.

3. Results and discussion

3.1. TCO properties and loss analysis

The electrical resistivity of the AZO layers at room temperature was found to be $5 \pm 1^{*}10^{-4}$ Ωcm as measured directly after the deposition, where the variation mainly depends on the base pressure in the deposition chamber (base pressure $5–10^{*}10^{-7}$ mbar measured with an ion gauge). The resistivity of the i:ZnO was measured to be more than seven orders of magnitude higher than that of the doped oxide. This was achieved not only by using an undoped ceramic target but also by an increased oxygen content in the sputter gas. Some sputtering and layer parameters are listed in Table 1. The sputter gas composition was tuned by mixing Ar and $Ar + O_2$ (3%) (the sputter gas composition values in Table 1 were determined out of the flux ratios). The resistivity of the i:ZnO is similar to values reported for intrinsic SnO_2 [2] and intrinsic ZnO layers grown for CIGS solar cell application [3,4]. After each processing step the resistivity of the AZO was re-measured using the metallic contact stripes. Since the resistivity of the subsequent layers i:ZnO, CdS and CdTe is with $1.0^{*}10^{4}$ Ωcm, $>4.0^{*}10^{2}$ Ωcm, and $7^{*}10^{2}$ Ωcm orders of magnitudes higher, their contribution can be neglected in the measurement procedure. No change of the resistivity was observed after any processing step. With ITO, in contrast to this we observed an increasing free carrier absorption in coincidence with decreasing resistivity which had negative effects on the short circuit current density and reproducibility.

To get a measure for the roughness of the ZnO layers atomic force microscopy (AFM) measurements were taken of AZO, AZO/i:ZnO, and FTO (for comparison) layers on glass substrates. The average surface roughness values S_a are summarized in Table 1. The surface of the AZO layer is found to be smoother than the surface of the FTO. The additional i:ZnO layer does not change the surface roughness of the AZO sample (Table 1).

In order to quantify the optical losses related to the TCO in the finished device transmission and reflection measurements of the single layers were performed and compared to the spectral response of the solar cell (Fig. 1). The losses were calculated by integrating the indicated regions weighted with the AM1.5G solar spectrum over the relevant wavelength range. Sites [5] has also analysed losses in CdTe solar cells to identify the limitations imposed by different layers in solar cell. Similar data for NREL's high efficiency CdTe solar cell was presented by Wu [6].

The free carrier absorption in the AZO leads to a loss of 1.2 mA/cm^2 in the short circuit current density (range 400–840 nm) in our solar cells. The loss could be reduced by increasing the electron mobility of the AZO layer without adversely affecting the resistivity [7]. Another 0.6 mA/cm^2 in the J_{SC} are lost in the AZO due to absorption of photons with energy above the energy band gap (E_g^{TCO}).

Table 1
Sputter gas composition, sputter power density used for AZO and i:ZnO deposition and layer resistivity and roughness.

	Ar/O2 [%]	Power density [W/cm^2]	ρ [Ω·cm]	Avg. roughness [nm]
i:ZnO	1.1	1.85	1.0E+4	12.7 (on AZO)
AZO	0.05	2.47	5.5E−4	12.4 (on glass)
FTO	–	–	6.0E−4	19.0 (on glass)

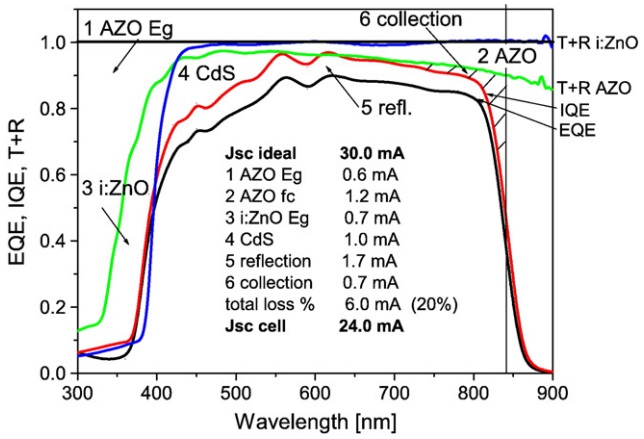

Fig. 1. Loss analysis of a CdTe solar cell with 60 nm CdS grown on AZO/i:ZnO TCO without anti reflection coating. Transmission plus reflection curves were measured on individual layers on glass. The internal and external quantum efficiency was obtained by averaging 5 curves.

The additional i:ZnO layer results in further 0.7 mA/cm^2 loss of the current density. However, this has to be put into perspective with the thereby facilitated thickness reduction of the CdS layer. The implementation of the i:ZnO layer reduced the parasitic absorption losses in the CdS layer to 1.0 mA/cm2 (see Fig. 4).The main current gain compared to earlier cells on FTO coated glass substrates without an intrinsic layer (see Table 3) originates from thinner CdS which is enabled by the HRT layer and the reduced roughness [8]. The beneficial effects in maintaining high open circuit voltage (Voc) have also to be considered for cells with i:ZnO layers (see Fig. 5).

3.2. The ZnO/CdTe junction

Because of non-conformal layer deposition of CdS and recrystallisation during the CdCl2 treatment of the CdS/CdTe stack, direct contacts between the TCO and the CdTe can locally occur due to island formation of the CdS and/or sulphur diffusion into the CdTe. This is even more pronounced if the initial CdS layer thickness is intentionally reduced. This means that locally the p–n junction is formed between the TCO and the CdTe semiconductors [9]. Those TCO–CdTe diodes are connected in parallel with the CdS–CdTe diodes and influence the device performance. In order to understand this influence on the performance, buffer free devices are investigated. We analysed the cases were the CdTe is in direct contact with the doped AZO and with the highly resistive i:ZnO. J–V characteristics of

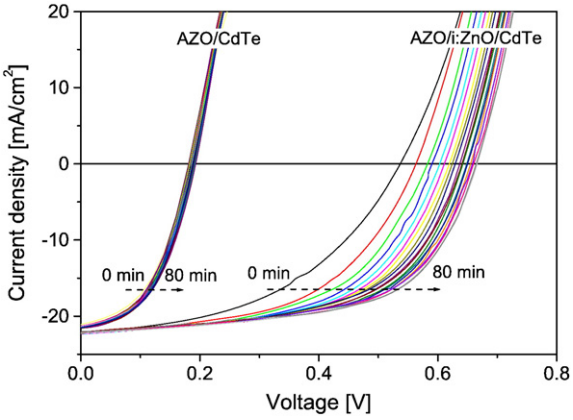

Fig. 2. Light soaking effect on i:ZnO/CdTe and AZO/CdTe heterojunction solar cells. While i:ZnO/CdTe exhibits strong light soaking AZO/CdTe does not change. The LS effect decays after illumination is stopped.

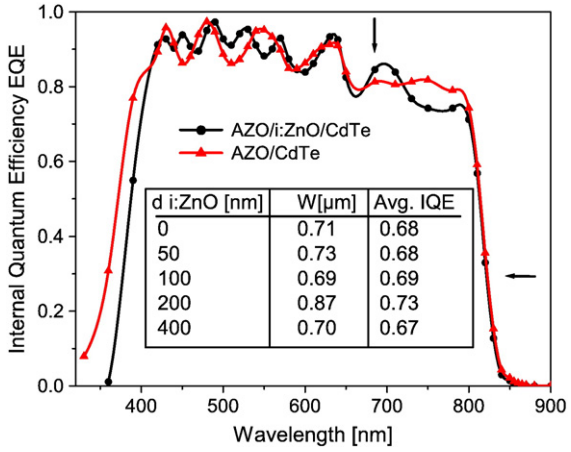

Fig. 3. Internal quantum efficiency of AZO/i:ZnO/CdTe (400 nm i:ZnO) and AZO/CdTe heterojunction solar cells. The much higher donor doping of AZO does not affect the carrier collection and the space charge region. Inset table: d i:ZnO = thickness of i:ZnO [nm], W = depletion layer width [µm], and Avg. IQE = averaged internal quantum efficiency (685–830 nm) as indicated with two arrows.

such devices are shown in Fig. 2 and IQE curves are plotted in Fig. 3. The corresponding photovoltaic parameters are given in Table 2.

The AZO/CdTe solar cells show a very poor initial performance with V_{OC} of about 180 mV and FF of 46%. No significant change is observed after 80 min of light soaking under white light illumination and open circuit condition. The initial performance of AZO/i:ZnO/CdTe solar cells is superior due to a higher V_{OC} of about 530 mV. A strong reversible light soaking effect is observed for the i:ZnO/CdTe solar cells increasing V_{OC} by 130 mV and FF by 13% absolute after 80 min illumination.

The IQE curves of the two devices are almost identical (Fig. 3). The CdTe absorption edges overlap perfectly. In both structures there is no CdS present and hence no effect due to the $CdTe1_{-x}S_x$ intermixing phase can be found. The CdTe band gap at 300 K for both CdS free structures derived from EQE is 1.487 ± 0.003 eV (average of five measurements). The response edge in the low wavelength part, which is caused by TCO absorption, differs due to the Burnstein–Moss effect which increases the optical band gap of doped AZO compared to the i:ZnO layer.

The C–V measurements performed at 300 kHz and 300 K revealed a comparable size of the depletion width (0.7 ± 0.1 µm) for all AZO/CdTe and AZO/i:ZnO/CdTe devices. The comparable junction characteristic is confirmed by the similar average IQE in the long wavelength part (Fig. 3, inset table).

A similar beneficial effect of the highly resistive i:ZnO layer was observed by Chaisitsak et al. [3] and Olsen et al. [4] for CdS free ZnO/CIS and ZnO/CIGS devices grown in substrate configuration. The device structures (ZnO/CIGS and ZnO/CdTe) exhibit similar increase in V_{OC} with higher ZnO resistivity and show similar light soaking behaviour. In the case of superstrate CIGS thin film solar cells with ZnO/CIGS junction a strong but irreversible light soaking effect has been reported by Haug et al. [10].

Table 2
IV parameters of AZO/CdTe and i:ZnO/CdTe devices initially and after 80 min of light soaking at room temperature.

	Voc [mV]	Jsc [mA/cm²]	FF [%]	Eff. [%]
AZO/CdTe	184	22.4	46.45	1.9
80 min LS	188	22.8	48.74	2.1
i:ZnO/CdTe	536	22.3	46.14	5.5
80 min LS	661	22.2	59.12	8.7

As the superior performance with high ZnO resistivity compared to low resistivity is observed for all three devices (ZnO/CIS, ZnO/CIGS and ZnO/CdTe) there might be one explanation for all three devices.

Olsen et al. [4] explained the beneficial effect of the high resistive ZnO with a reduced recombination rate at and near the ZnO/CIS interface. With the assumption that the higher resistivity of the ZnO increases the carrier lifetime he demonstrated increasing efficiency with increasing ZnO resistivity by 1D model calculations. Chaisitska [3] assumes as well that a reduced recombination rate at the interface might be responsible for the beneficial effect of high resistive ZnO in ZnO/CIGS devices.

We performed simple straight forward simulations (no defects at interfaces) with SCAPS [11] which showed the opposite behaviour (increasing performance with decreasing buffer resistivity) for CdTe/ZnO. But by introducing acceptor defects at the ZnO/CdTe interface, the behaviour as observed in the experiment occurred also in the simulation. The presence of interface defects seems feasible as ZnO exhibits a large lattice mismatch of 20% to CdTe [12]. According to the simple Anderson model the CdTe/ZnO interface exhibits a negative conduction band offset (−0.4 eV [12,13]) which could also increase the recombination rate at the interface.

3.3. Thin buffer: CdS/CdTe and ZnO/CdTe in parallel circuit

The thickness of the CdS layer in the CdS/CdTe device is an important parameter for performance optimization. Since electron hole pairs generated in the CdS layer are very inefficiently collected, the CdS layer leads to absorption losses. In order to minimise these optical losses the thickness of the CdS layer should be as thin as possible. However, there is a trade-off between current gain and voltage as well as FF losses when reducing the CdS thickness. The voltage and FF drop can be reduced by introducing a high resistive layer between the TCO and the CdS [2]. We investigated the influence of CdS and i:ZnO layer thicknesses on the device performance in detail.

The influence of the CdS layer thickness on the J_{SC} was investigated by analysing a set of averaged quantum efficiency curves shown in Fig. 4.

A reduction of the CdS layer thickness increases the J_{SC} by reducing optical losses (arrow 1). Simultaneously the carrier collection is slightly reduced (arrow 2). In the case of the omitted CdS layer the reduced collection efficiency leads to a similar reduction in Jsc as the

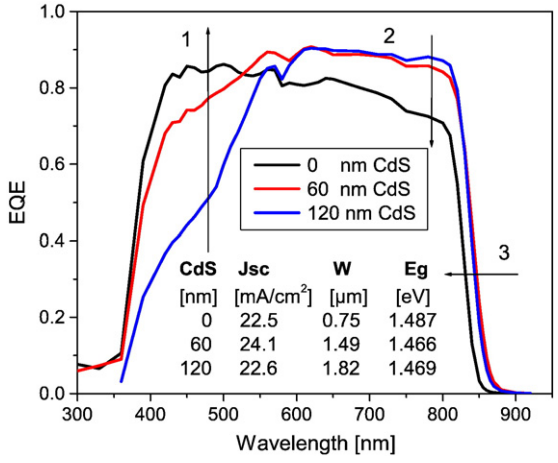

Fig. 4. External quantum efficiency curves of CdTe solar cells with 0 nm, 60 nm and 120 nm CdS layer thickness. The arrows indicate three effects: 1: increasing short wavelength response due to reduced CdS absorption; 2: decreased collection probability of "red" photon generated electrons due to decreasing W with thinner CdS; and 3: change in CdTe absorption edge (minimum bandgap) due to CdS/CdTe intermixing. Inset: Current density — Jsc, depletion layer width — W and CdTe minimum bandgap — Eg.

optical absorption of the 120 nm thick CdS layer. Intermixing of CdS–CdTe is expected to change the energy gap of CdS–Te and CdTe–S alloys depending on the composition. The respective values of the ternary compound are lower due to bandgap bowing [14]. The CdS/CdTe intermixing decreased the CdTe band gap compared to the ZnO/CdTe device from 1.487 ± 0.003 eV to 1.467 ± 0.003 eV which leads to a potential current gain of 0.74 mA/cm^2 (arrow 3).

The open circuit voltage of devices without the i:ZnO layer strongly depends on the CdS thickness (Fig. 5). Similar observations were reported by Li et al. for SnO_2 based TCOs [2]. Fig. 5 shows as well that the V_{OC} of the devices with different CdS thicknesses is independent of the i:ZnO layer thickness over the range from 50 nm–200 nm but at 400 nm the voltage drops slightly.

As mentioned above, direct contacts between the TCO and the CdTe can locally occur due to island formation of the CdS layer and/or sulphur diffusion into the CdTe after the recrystallisation treatment [9]. The CdTe solar cells with CdS buffer layer thickness below 200 nm (the exact value depends on the TCO roughness, CdS deposition technique and the recrystallisation treatment) can hence be interpreted as a parallel connection of several ZnO/CdTe and CdS/CdTe junctions. With decreasing CdS thickness the contribution of the direct ZnO/CdTe junctions increases. The higher V_{OC} of devices with the i:ZnO layer can be explained with the higher voltage the i:ZnO/CdTe junction generates compared to the AZO/CdTe interface.

Rau et al. [15] explained the beneficial effect of a HRT layer in thin film solar cells with electronic loss restriction. They showed that a HRT layer improves the V_{OC} and FF by limiting the current flow back into weak diodes.

We suggest that both effects, the higher voltage at the i:ZnO/CdTe junction and the restriction of current flowing back into weak diodes, are responsible for the beneficial effect of the i:ZnO layer in CdS/CdTe solar cells.

With increasing i:ZnO layer thickness a reduction of the internal QE in the long wavelength part (685–830 nm) could be observed (Fig. 6a). Capacitance measurements revealed a decreasing depletion layer width (W) with increasing i:ZnO layer thickness as shown in Fig. 6b.

The dependence between the i:ZnO thickness and the depletion width seems to follow a logarithmic relation. A physical explanation has still to be found.

The effect of the i:ZnO layer on the short circuit current density is shown in Fig. 7 and can be summarized as follows. (i) Implementation of an i:ZnO layer increases the depletion width and with it the collection in the long wavelength region. With increasing i:ZnO layer thickness the depletion width shrinks and the collection efficiency, i.e. the J_{SC} decreases again. (ii) Parts of the UV-spectrum are lost due to a direct band gap of 3.2 eV of the i:ZnO layer, which results in a potential current loss of 0.7 mA/cm^2 (see Fig. 1). It can be concluded that the beneficial effect of the i:ZnO by far outweighs the additional optical losses. For optimum performance the thickness should be chosen below 100 nm.

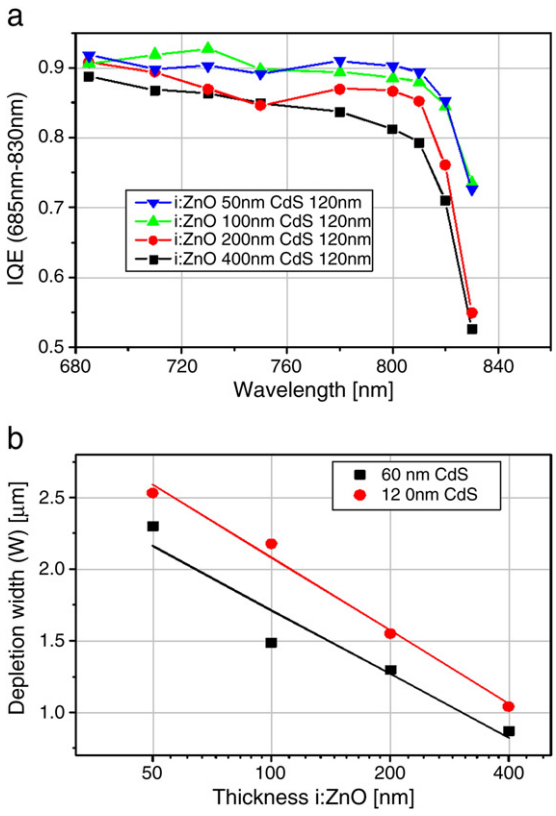

Fig. 6. Influence of the i:ZnO layer thickness on carrier collection and depletion layer width (W). The internal quantum efficiency in the long wavelength part (685 nm–830 nm) is reduced with increasing i:ZnO thickness (a).The depletion layer width decreases with a thicker i:ZnO layer (b). The reduced carrier collection (a) seems to be a consequence of the reduced W (b).

3.4. Cells with AZO front contact on various substrates

Table 3 gives an overview over the PV parameters of CdS/CdTe solar cells grown by low temperature evaporation processes on a

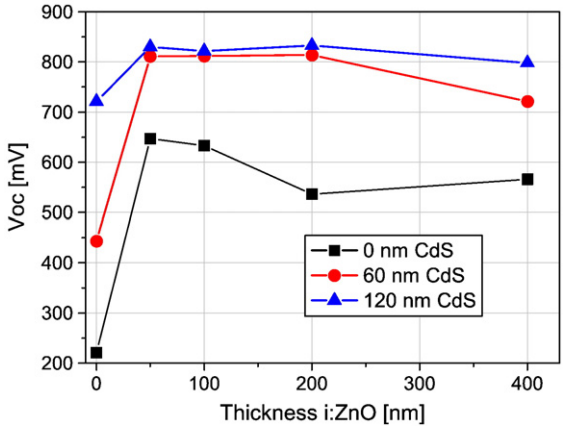

Fig. 5. V_{OC} of CdTe/CdS devices with different CdS and intrinsic layer thicknesses. Implementing a thin intrinsic layer significantly increases the cell voltage. Thick intrinsic layers decrease the cell voltage slightly compared to thinner layers.

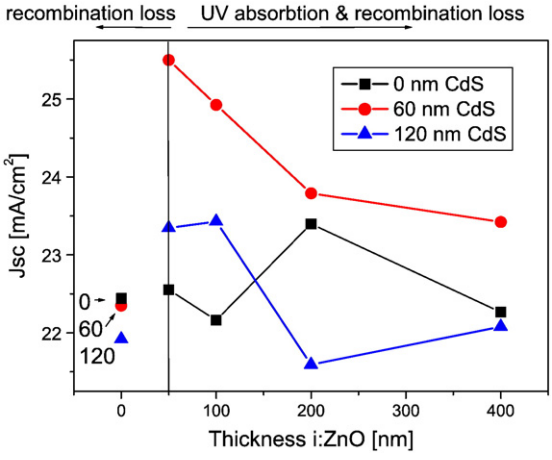

Fig. 7. Short circuit current density derived from quantum efficiency measurement as a function of the i:ZnO layer thickness. The current density is influenced by UV absorption and collection losses.

Table 3
Parameters of the solar cells produced on various substrates with AZO/i:ZnO bilayer front contact. For comparison the best cell on FTO is also included.

Substrate	Voc [mV]	Jsc [mA/cm²]	FF [%]	Eff. [%]	Remarks
ASG	834	24.7[a]	75.9	15.6	90 nm CdS
BSG	821	25.0[a]	74.8	15.4	60 nm CdS
SLG no barrier	821	22.9	72.4	13.0	120 nm CdS, low yield
PI 7.5 μ	823	19.6	76.5	12.4	120 nm CdS
PI 12.5 μ	799	17.8	72.2	10.3	120 nm CdS
Tec 15 (FTO)	826	20.1	73.0	12.1	350 nm CdS
BSG/Mo	658	21.4	61.2	8.6	Substrate configuration

[a] Anti reflection coating applied.

variety of substrates using AZO/i:ZnO bilayer front contact. Solar cells with 15.4% and 15.6% efficiency have been obtained on borosilicate and aluminosilicate glass, respectively. Slightly lower efficiency of 13.0% was achieved on soda-lime glass (SLG) without additional barrier for alkaline metals. Although AZO/i:ZnO is a barrier against alkali metal diffusion as others observed for CIGS grown in superstrate configuration [10] this barrier turned out to be insufficient for CdTe solar cells on SLG. The yield on the SLG substrate is also significantly reduced, which can be linked to sodium diffusion (white spots visible on cells with reduced efficiency). The detailed results about sodium tolerance of CdTe solar cells on AZO/i:ZnO coated substrates will soon be published.

On flexible polyimide (PI) excellent PV performance of the solar cells with efficiency above 12% is measured [16]. Efficiencies above 10% on PI with AZO front contact was recently also reported by Vasko et al. [17]. The main advantages compared to the ITO used in earlier work [18] were significantly reduced wrinkling, higher yield, and improved cell parameters.

The use of steel, aluminium, or other cheep metal foils is still hindered by the lack of a suitable back contact for the substrate configuration. With a Mo/Sb_2Te_3 back contact on the ASG substrate the best cell grown by the low temperature evaporation method in our lab showed 8.6% efficiency.

4. Conclusion

AZO layers with 1 μm thickness can be prepared with a stable sheet resistance of 5 Ω□ by adjusting the sputter parameters. The optical losses in the AZO layer due to free carrier absorption lead to a loss in J_{SC} of 1.2 mA/cm^2. This is about twice the losses reported for cadmium stannate; however, it is still significantly lower than the losses reported for FTO [5,6]. The surface of the AZO/i:ZnO bilayer was found to be smoother than commercially available FTO. The AZO/i:ZnO/CdTe heterojunction shows a much higher V_{OC} than AZO/CdTe which explains the beneficial effect of the intrinsic layer in case the coverage of the CdS layer is incomplete resulting in direct TCO/CdTe contacts. Increasing thickness of the intrinsic layer was not found to increase the yield; however, it reduces the J_{SC} due to reduced UV transmission and depletion width of the junction. Best efficiency was obtained with intrinsic layer thickness between 50 nm and 100 nm. Solar cells with efficiencies of 15.6% on glass and 12.4% on flexible PI were achieved using AZO/i:ZnO bilayer front contact and our low temperature deposition processes.

References

[1] A. Gupta, A.D. Compaan, Appl. Phys. Lett. 85 (2004) 684.
[2] R.R. X. Li, National Center for Photovoltaics Program Review Meeting, Denver Co (US), 1998.
[3] S. Chaisitsak, T. Sugiyama, A. Yamada, M. Konagai, Jpn. J. Appl. Phys. 38 4989.
[4] L.C. Olsen, Photovoltaic Specialists Conference, 1996. Conference Record of the Twenty Fifth IEEE Washington, DC, 1996, p. 997.
[5] J.R. Sites, Sol. Energy Mater. Sol. Cells 75 (2003) 243.
[6] X. Wu, Sol. Energy 77 (2004) 803.
[7] K. Ellmer, J. Phys. D Appl. Phys. 34 (2001) 3097.
[8] A. Romeo, G. Khrypunov, F. Kurdesau, M. Arnold, D.L. Bätzner, H. Zogg, A.N. Tiwari, Sol. Energy Mater. Sol. Cells 90 (2006) 3407.
[9] M. Terheggen, H. Heinrich, D. Baetzner, A. Romeo, A.N. Tiwari, Interface Sci. 12 (2004) 259.
[10] F.J. Haug, D. Rudmann, H. Zogg, A.N. Tiwari, Thin Solid Films 431–432 (2003) 431.
[11] M. Burgelman, P. Nollet, S. Degrave, Thin Solid Films 361–362 (2000) 527.
[12] B.K. Meyer, A. Polity, B. Farangis, Y. He, D. Hasselkamp, T. Kramer, C. Wang, Appl. Phys. Lett. 85 (2004) 4929.
[13] S.-H. Wei, A. Zunger, Appl. Phys. Lett. 72 (1998) 2011.
[14] A. Luque, S. Hegedus, Handbook of Photovoltaic Science and Engineering, John Wiley and Sons, 2003.
[15] U. Rau, M. Schmidt, Thin Solid Films 387 (2001) 141.
[16] J. Perrenoud, S. Buecheler, A.N. Tiwari, Proc. SPIE 7409 (2009) 7490L.
[17] A.C. Vasko, X. Liu, A.D. Compaan, 2009 34th IEEE Photovoltaic Specialists Conference, Philadelphia, PA, 2009, p. 001552.
[18] G. Khrypunov, A. Romeo, F. Kurdesau, D.L. Bätzner, H. Zogg, A.N. Tiwari, Sol. Energy Mater. Sol. Cells 90 (2006) 664.